SLAC-PUB-2120
May 1978
(E)

PRODUCTION OF LEPTONS AND LEPTON PAIRS IN $\pi^{\pm}$p INTERACTIONS*

R. F. Mozley
Stanford Linear Accelerator Center
Stanford University, Stanford, California 94305

INTRODUCTION

Two low sensitivity but excellent mass resolution lepton production experiments are reported on, both performed at SLAC.

One is a study of e± production in π^- interactions at 18 GeV/c performed using the SLAC hybrid bubble chamber. The other is a study of muon pair production in 15.5 GeV/c π^- interactions.

e PAIR EXPERIMENT

The $e^{\pm}$ experiment was performed by the following persons: (SLAC) J. Ballam, J. Bouchez, T. Carroll, G. Chadwick, V. Chaloupka, C. Field, D. Freytag, R. Lewis, K. Moffeit, and R. Stevens; (Duke University) H. Band, L. Fortney, T. Glanzman, J. S. Loos, and W. D. Walker; (Imperial College) P. A. Baker, P. J. Bornan, D. J. Gibbs, G. Hall, A. P. White, and T. S. Virdee. It utilized a large number of techniques for identification of electrons, in particular the introduction of three one-radiation-length tantalum plates into the hydrogen bubble chamber. Figure 1 shows a photograph of an electron pair event in the

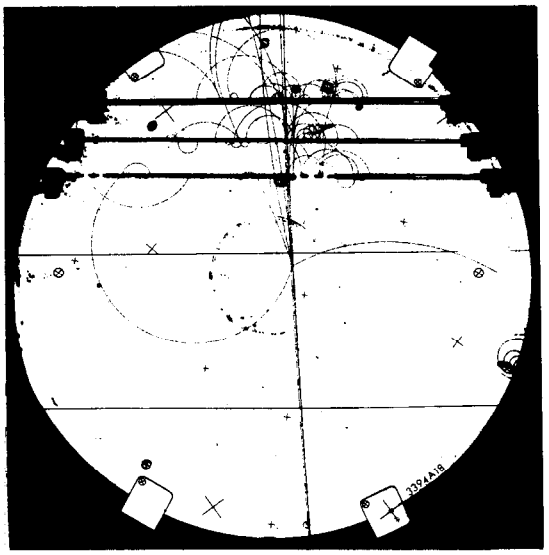

Fig. 1. Bubble chamber photograph

*Work supported by the Department of Energy.
(Invited talk presented at the 3rd International Conference at Vanderbilt on New Results in High Energy Physics, Nashville, Tenn. March 6-8, 1978).

chamber. The following methods were used for electron identification;

1. Spiralling (for tracks down to 1 MeV/c).
2. Bremsstrahlung in hydrogen.
3. High energy delta rays.
4. Ionization (useful to $\sim$ 200 MeV/c).
5. Interactions in the plates.

Criteria for electron identification based on studies with an electron beam were:

a. Electrons interact visibly before third plate.
b. Transverse momentum of tracks in the electron shower does not exceed 30 MeV/c.
c. No track with momentum > 10 MeV/c at $\theta > 90^{o}$.
d. Total E_{vis} in shower behind at least one plate > 7% of incoming.
e. No hadron signature (i.e., heavy ionization, stub tracks, etc.)

The 4π solid angle and selective criteria allowed a study of single electron production with 10^{-4} discrimination from hadrons.

An exposure of 250,000 πp interactions was made and resulted in the following number of events:

A. Single $e^{\pm}$ candidates with all other tracks identified as hadrons. 22 events.
B. Candidates in pairs, from 55% of the data available so far. 2,000 pairs.
C. Single $e^{\pm}$ candidates with at least one unidentifiable track of opposite charge, from 55% of the data available so far. 400 pairs.

The analysis of the apparent electrons produced without an opposite charge partner made use of a study of the properties of pion induced showers in the plates. For this, pure beams of pions at 1.57 and 3.14 GeV/c were used, and a background level was established for pions to simulate electron showers (at about 1 in 2×10^{4} pions).

The 22 single electron candidates corresponded by themselves to an e/π ratio of $(4.3 \pm .9) \times 10^{-5}$. All the properties of the events were consistent with the hypothesis of pion breakthrough, and subtracting the measured rate of breakthrough a limit on direct, unpaired, electron production was obtained: $e/\pi < 2.4 \times 10^{-5}$ at 90% C.L.

From this a limit on charmed particle production could be derived in terms of the semi-leptonic branching ratios. Using the recent measurement for the electron decays of the D mesons, the limit is $\sigma < 13$ μb at 90% C.L. This indicates that virtually all of the reported electrons in hadronic interactions are from pair production.

A study of the production of positron electron pairs was also performed. Here the small number of interactions made the experiment sensitive only to very low mass pairs, mostly lower than the π^{o} mass. The results were again compared with the detailed Monte Carlo calculation. Pair production from all known sources was introduced using the following production cross sections:

η	σ = 1.3 mb	
ω	σ = 3.4 mb	
ρ	σ = 4.0 mb	(Ref. 1)
$\pi^{\pm}$	σ = 85 mb	
π^{o}	σ = 36 mb	

The results are compared in Tables I and II.

Table I A Comparison of the p_t Distribution of e^+ and e^- Tracks with That Expected from a Monte Carlo Calculation Encompassing All Known Sources

(A)

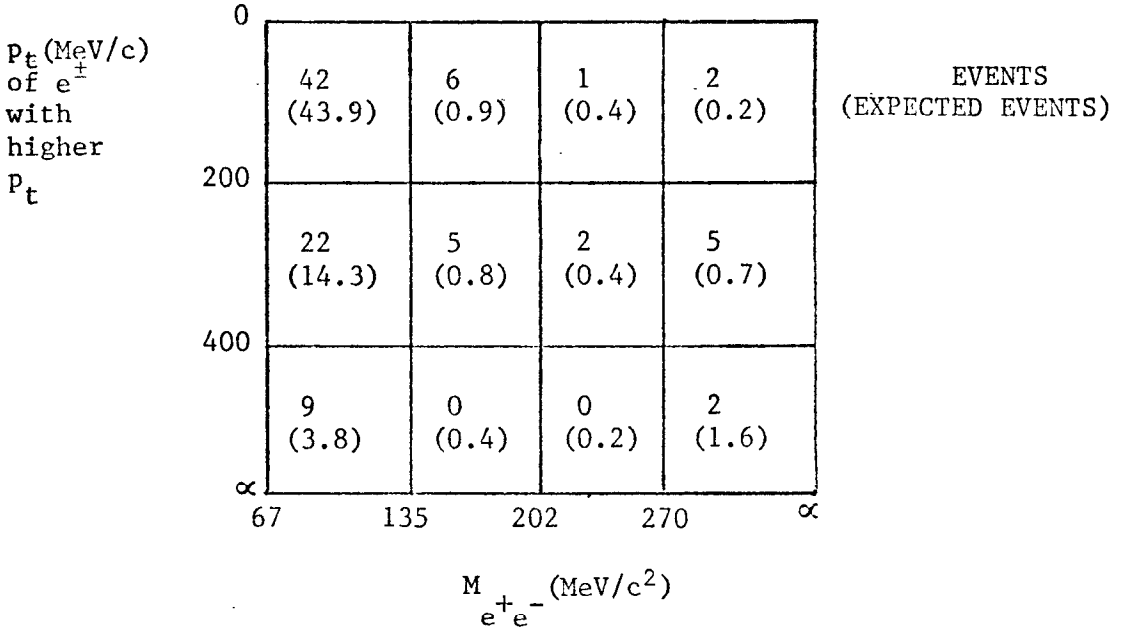

(B)

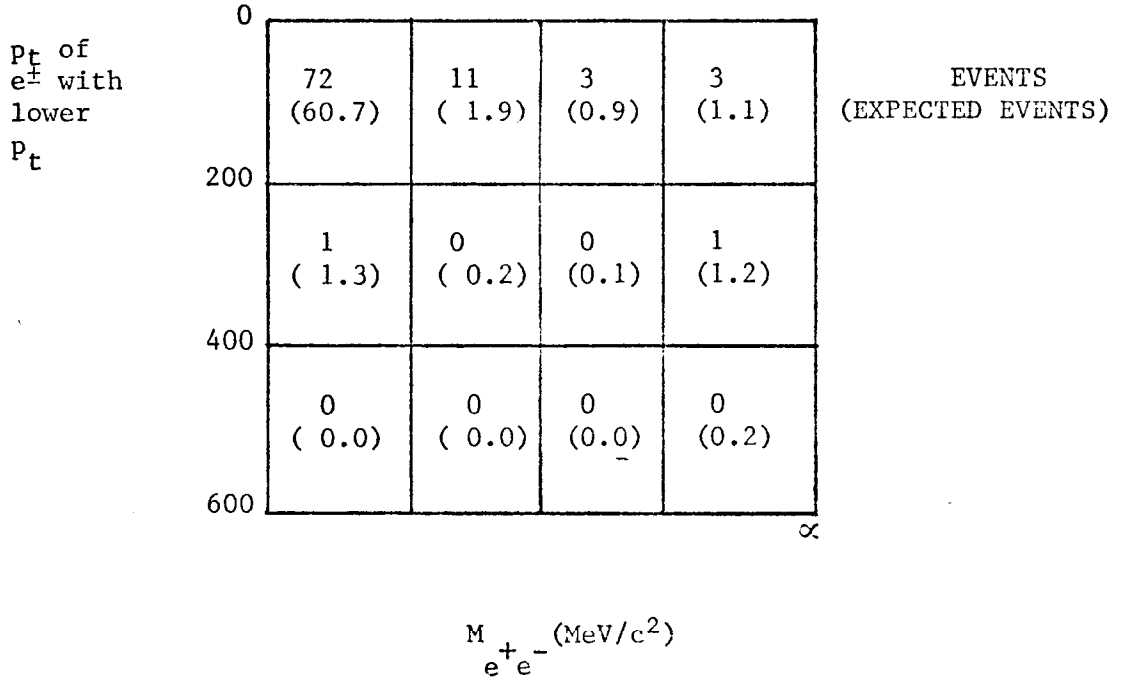

Table II The Excess of Measured $e^{\pm}$ Tracks Over Those Predicted by a Monte Carlo Calculation Encompassing all Known Sources. Both e^+ and e^- are Counted

p_t (MeV/c) of e^+ or e^-	OBSERVED -MONTE CARLO $M_{ee} > 67$	$M_{ee} > 135$	Expected at $\pi^{\pm}$ rate $\times 10^{-4}$
0	35.0 $\pm$18.0	25.7 $\pm$5.6	13.4
200	11.0 $\pm$6.1	9.5 $\pm$3.7	15.6
400	4.3 $\pm$3.5	-0.4 $\pm$1.5	14.2

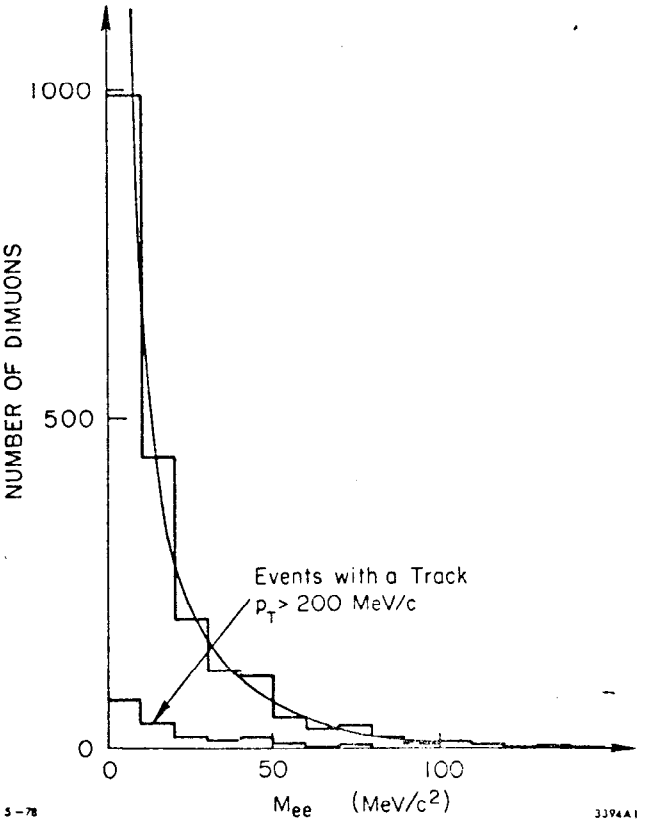

Fig. 2. Mass plot

A mass plot is shown in Fig. 2. This indicates the agreement between the Monte Carlo, including resolution, and the π^o Dalitz pair dominated pair spectrum. Only above 135 MeV/c^2 is the data strong enough to indicate a significant excess of pairs. The excess of electrons and positrons in this mass range tend to cluster at low p_T (Table II).

μ PAIR EXPERIMENT

The μ pair production experiment was performed using 15.5 GeV/c $\pi^{\pm}$ beams incident on a liquid hydrogen target in the SLAC two-meter streamer chamber. The collaboration involved was the following:

SLAC: K. Bunnell, M. Duong-van, E. Kogan, B. Haber, R. Mozley, A. Odian, F. Villa, L. Wang.

Vanderbilt: R. Cassell, R. Panvini, S. Poucher, A. Rogers, S. Stone.
U.C.S.C. : T. Schalk.
M.I.T. : W. C. Barber

The results reported here are from an exposure of 10^8 πp interactions which yielded 335 pairs with $X_F > 0.3$. This is half of the total exposure the rest of which is being analyzed.

The experimental layout is shown in Fig. 3. The pion beam is incident from the left into a 3cm diameter one-meter-long liquid hydrogen target mounted inside the visible region of the streamer chamber. The chamber is mounted in a 13 Kgauss magnet and viewed from above in three camera stereo. Directly downstream of the chamber a hadron absorber of copper and lead is erected with a hole allowing passage of the noninteracting pions in the beam. A scintillation counter hodoscope is interspersed in the wall with horizontal counters A, C, and E and vertical counters B and D. A trigger consisted of an interaction in the hydrogen target (i.e., a particle-incident and non-emergent) and the firing of a pair of appropriately lined up A and C counters and two nonadjacent B counters. The system would trigger on particles of momenta greater than 2 GeV/c. Hits on the D, E, and F scintillation counters were recorded as well as those in two wire chamber planes(W).

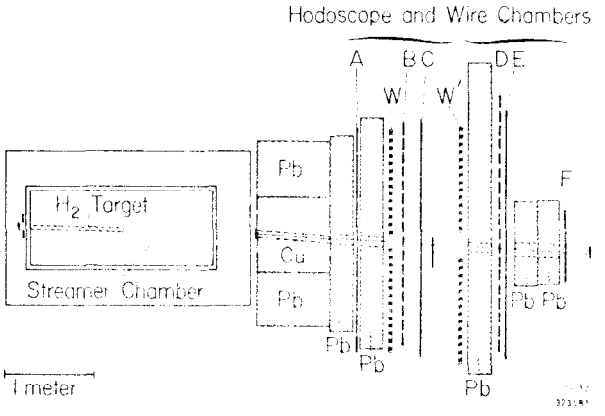

Fig. 3. Plan view of streamer chamber

Fig. 4. Streamer chamber photograph with muon candidates (tracks 1, 2, and 3.)

Figure 4 shows a photograph of a muon pair candidate in the streamer chamber. Hadron punch-through was reduced by the following procedure: Muon candidate tracks such as 1, 2, and 3 were measured in the streamer chamber and extrapolated positions calculated at the counter and wire chamber locations. A measured position over three standard deviations from the projected position was taken as evidence that the particle was in fact a hadron.

Figure 5a shows a plan view of three muon candidates visible in Fig. 4. All of the tracks satisfy muon criteria in this view. Fig. 5b shows a side view of the same three tracks. There is no appropriate hit for track 2 in the first plane of wire chambers, and as a result tracks 1 and 3 are identified as muons and track 2 as a hadron.

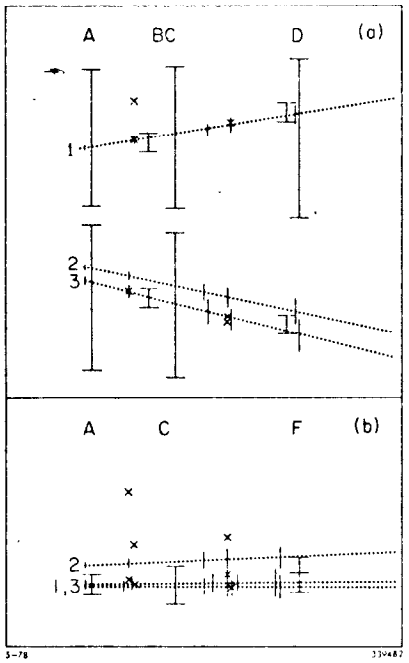

Fig. 5a. Plan view of arrangement of downstream scintillation counters and wire chambers. The location of counters hit is shown by lines with horizontal bars I while the predicted track location is shown by lines without horizontal bars which extend ± 1 σ; wire chamber hits are shown by crosses. 5b. Side view of arrangement of downstream counters and wire chambers.

To calculate the punchthrough expected with the use of these criteria, an exposure was made to events resulting from beam interactions and another exposure to events with a single muon trigger. The particles causing single muon triggers are primarily hadrons ∿ 30/1 and hence can serve as an excellent model for hadron punchthrough. As a result the muon candidate tracks from the single muon events were measured and subjected to the same scrutiny as that for the two muon trigger events. These were then treated as examples of hadron punchthrough and the hadron punchthrough probability calculated as a function of energy. The interaction trigger events were measured and used as a sample of the hadrons incident on the lead wall. The measured punchthrough probability was applied to single muon events and the probability of their simulating dimuons was then calculated.

It was found that excessive punchthrough occurred if all events were used which penetrated through to the C counters (2 GeV/c particles), and as a result the events reported on here had muon candidates which registered as passing through enough lead to reach the D and E counters. The minimum momentum required for this was 2.4 GeV/c. This resulted in a minimum X_F of 0.3. Figure 6 shows the acceptance for X_F (c of m momentum in beam direction/maximum possible c of m momentum) and dimuon mass.

Table III summarizes the data obtained while Fig. 7 shows the dimuon mass spectrum. A clear ω signal can be seen, plus a ρ signal and a considerable enhancement below the ρ. It was not possible to make a clean fit to the ρ signal without a better understanding of the nature of the background under it. Allowing the background to vary could give an excellent fit for a very large range of ρ cross sections and hence none is determined here. The calculated punchthrough background is shown crosshatched.

Estimates of the maximum size of $\eta \to 2\mu$ decay can be made because of the good mass resolution. For this purpose the mass binning is adjusted to allow a single bin to be centered on the m mass. An insignificant signal thus observed allows a cross section calculation to be made.

Table III. Data Summary

	π^+	π^-	Combined
Interactions	45.3×10^6	51.1×10^6	96.3×10^6
Sensitivity (events/μbarn)	1,880	1,990	3,870
Dimuons found (background) $\mu^+\mu^-$	137 (17)	198 (44)	335 (61)
$\mu^+\mu^+$	15 (8)	3 (9)	18 (17)
$\mu^-\mu^-$	1 (1)	22 (19)	23 (20)
Cross section observed $x_F \to 0.3$ (nanobarn)			
$\pi p \to \mu^+\mu^- X$	250 ± 70[a]	320 ± 90	280 ± 70
$\pi p \to \omega X \to \mu^+\mu^- X$			30 ± 13
$\pi p \to \eta X \to \mu^+\mu^- X$			3 ± 3
$\sigma(\pi^- p \to \mu^+\mu^- X)/\sigma(\pi^+ p \to \mu^+\mu^- X) = 1.28 \pm 0.23$		$\frac{\sigma(\mu^+\mu^-)}{\sigma(\pi^+\pi^-)} = (3 \pm 1) \times 10^{-5}$	

(a) This number can be compared with the value of 340 ± 70 obtained at 150 GeV/c.[6]

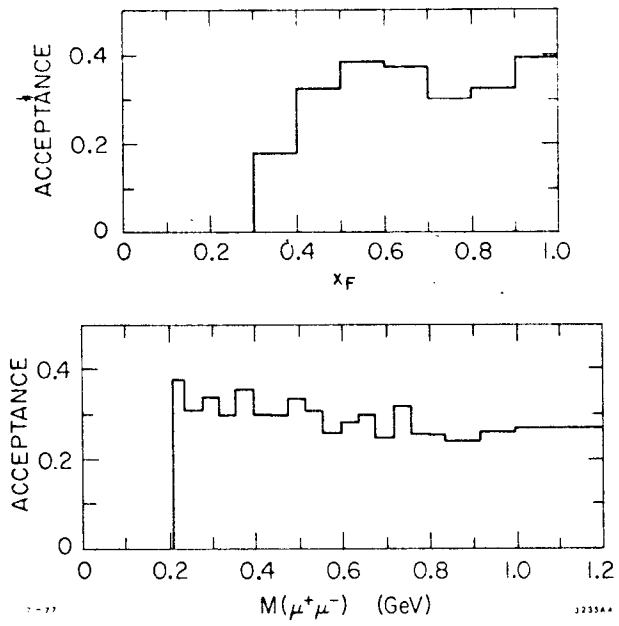

Fig. 6. Acceptance of the apparatus for dimuons.

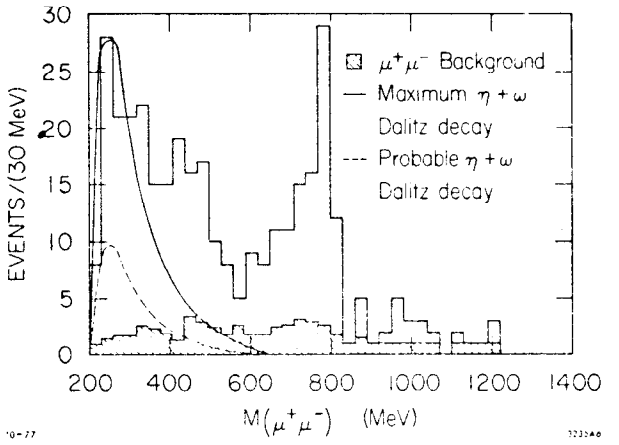

Fig. 7. Measured dimuon mass spectrum. Estimates of the hadron punchthrough background and contributions from η and ω Dalitz decay are indicated.

Figure 8 shows the mass spectrum with the background subtracted. The possible contribution from Dalitz decays of the η and ω can be estimated in two ways. One way is to use our measured values of η and $\omega \to 2\mu$ cross sections and to calculate their Dalitz decay contribution from this (Ref. 2). This is shown as the dotted curve in Fig. 7 and the mass spectrum with this and the background subtracted is shown in Fig. 9.

A more conservative way of estimating Dalitz decay backgrounds is to make use of the excellent mass resolution to introduce the maximum signal which could be present. This involves only knowing the shape of the Dalitz contribution, and here we use a shape with a very large ω contribution to emphasize the width of the distribution. The maximum possible contribution is shown in Fig. 7. If the contribution were larger than this it would cause the mass plot to peak at a higher value near threshold. The mass plot with the background and this maximum Dalitz contribution subtracted is shown in Fig. 10. Thus the good mass resolution allows this low statistics experiment to show for the first time model independent evidence for the existence of a dimuon mass continuum below the ρ which cannot be derived from Dalitz decay of known mesons.

There are an adequate number of theoretical papers predicting such behavior. A calculation by Bjorken and Weisberg (Ref. 3) produced a

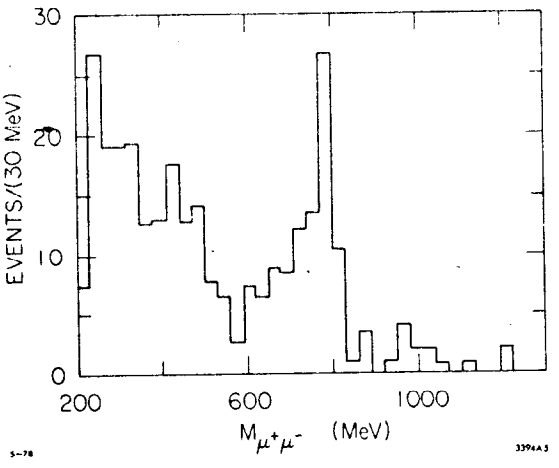

Fig. 8. Dimuon mass spectrum after subtraction of the calculated hadron punchthrough.

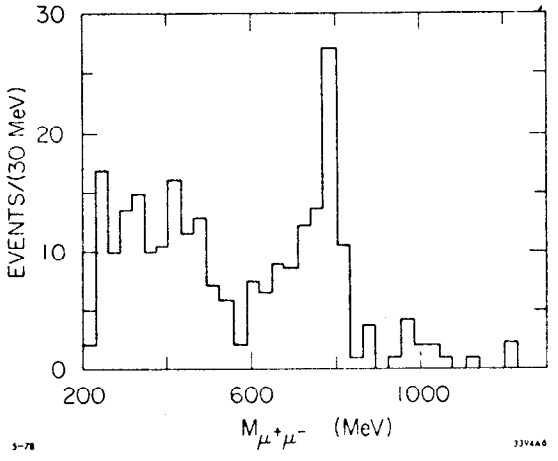

Fig. 9. Dimuon mass spectrum after subtraction of the calculated hadron punchthrough and the most probable contribution from η and ω decays.

qualitative enhancement here by quark antiquark annihilation similar to that predicted by the Drell-Yan model but enhanced by the annihilation with the additional quarks produced in pion production. Calculations by Blankenbecler and Duong-van (Ref. 4) of pion pion annihilation produced a phenomenological more quantitative estimate. A similar enhancement would occur from the pion bremsstrahlung prediction of Frautshi and Farrar (Ref. 5) but here we would expect a mass spectrum peaking more at threshold.

It is interesting to study the X_F spectrum as a function of the mass region. The result is shown in Fig. 11. The region of the ρ shows a flatter spectrum as would be expected from the known enhancement of ρ production at high X_F. The transverse momenta of the observed pairs is shown in Figs. 12 and 13. Differences between the mass regions are not statistically significant.

The decay angle of the muons with respect to the direction of the muon pair can be examined but unfortunately the acceptance of the trigger lessens the value of this. Muons produced at almost all c of m angles are incident on the lead absorber but those produced at large angles have insufficient energy to penetrate the lead. The acceptance is shown in Fig. 14. Figure 15 shows the resulting distribution. The results don't clearly differentiate between distributions although a $\sin^2\theta$ distribution is slightly preferred over $(1 + \cos^2\theta)$. The same data is shown in Fig. 16 broken up into different mass intervals. No statistically significant differences are observed.

Since the entire final state can be observed in the streamer chamber, it is interesting to examine the hadrons in the events to see if their characteristics differ from those in nondimuon events. To make

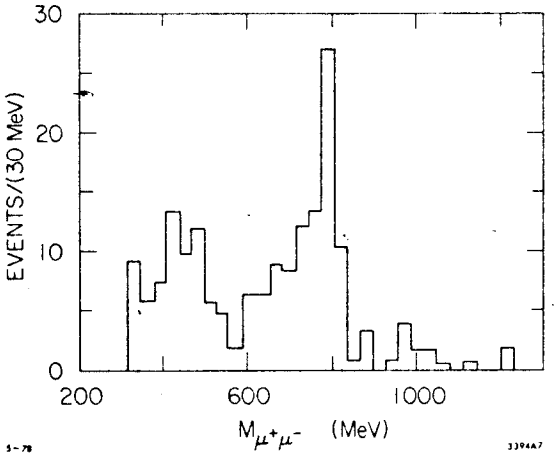

Fig. 10. Dimuon mass spectrum after subtraction of the calculated hadron punchthrough and the largest possible contribution from η and ω Dalitz decays.

Fig. 11a. X_F distribution of muon pairs with a mass between 200 MeV and 380 MeV.
11b. X_F distribution of muon pairs with a mass between 380 MeV and 600 MeV.
11c. X_F distribution of muon pairs with a mass between 600 MeV and 900 MeV.

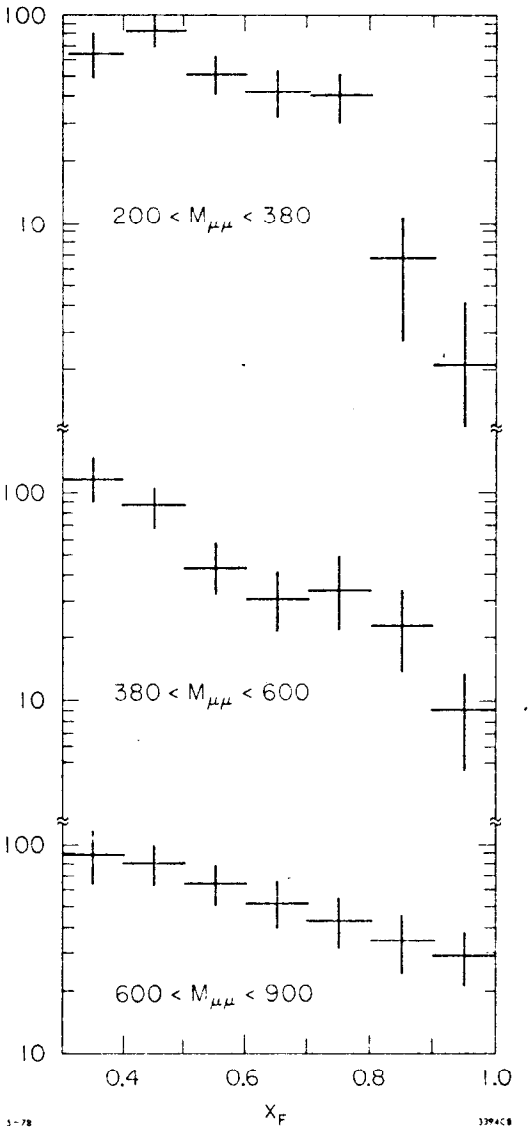

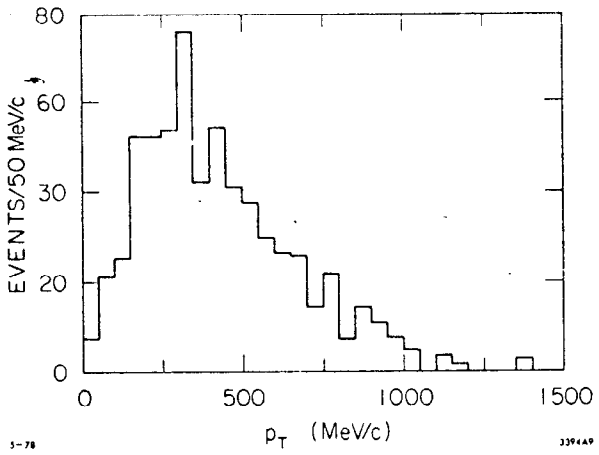

Fig. 12. Transverse momentum distribution of muon pairs $\langle p_T \rangle$ 420 MeV.

Fig. 13a. Transverse momentum distributions of muon pairs $200 < M_{\mu^+\mu^-} < 380$.
b. Transverse momentum distribution of muon pairs $380 < M_{\mu^+\mu^-} < 620$.
c. Transverse momentum distribution of muon pairs $620 < M_{\mu^+\mu^-}$

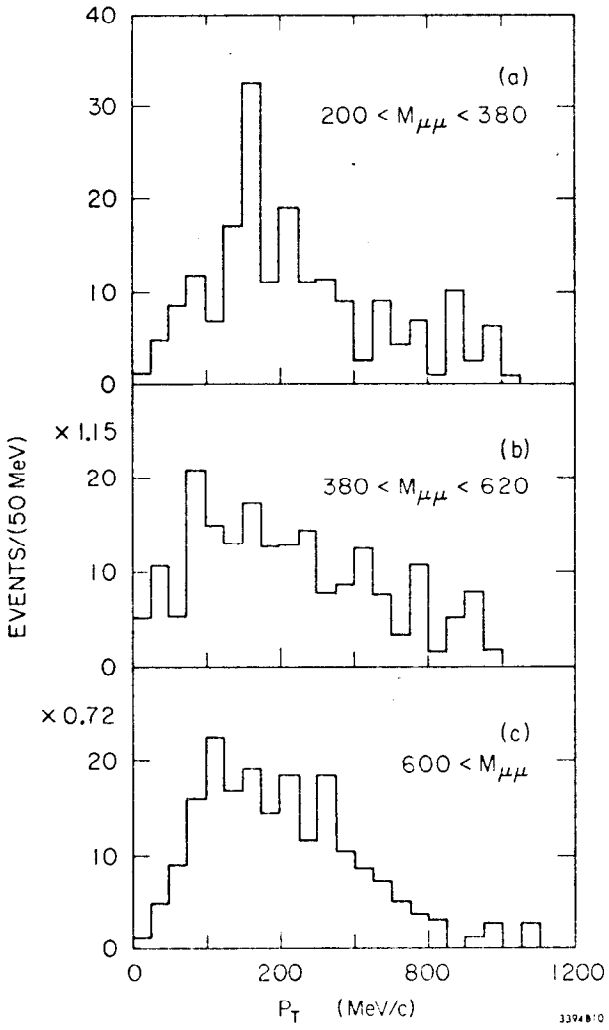

Fig. 14. Acceptance for muon pairs as a function of the decay angle of the μ^+ with respect to the pair direction in its c of m system.

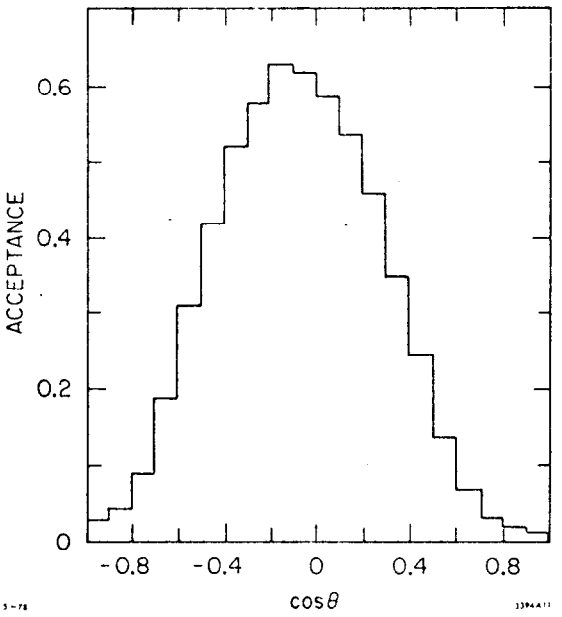

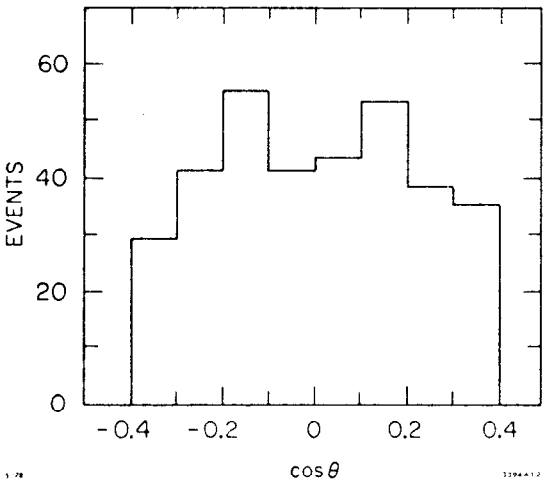

Fig. 15. Decay Distribution of μ^+ with respect to pair direction in its c of m system.

χ^2 for 4 Degrees of Freedom		
Flat	$\sin^2\theta$	$(1 + \cos^2\theta)$
7.1	4.6	10.3

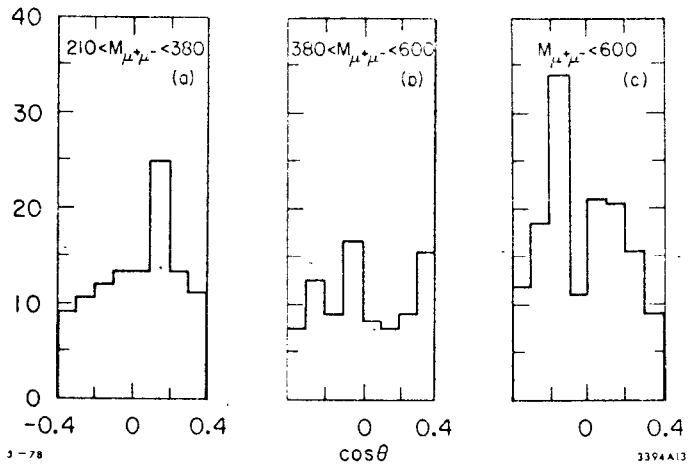

Fig. 16. Decay distributions for different $M_{\mu^+\mu^-}$ intervals.

χ^2 for 4 Degrees of Freedom

Flat	$\sin^2\theta$ $(1 + \cos^2\theta)$		Flat	$\sin^2\theta$ $(1 + \cos^2\theta)$		Flat	$\sin^2\theta$ $(1 + \cos^2\theta)$	
3.5	2.5	4.6	1.5	1.9	1.6	10.6	8.5	13.0

this comparison we use the interaction trigger events mentioned earlier with respect to our background calculations. For studies using these events we identify pions in the nondimuon events which would be possible muon candidates if a trigger had in fact occurred. Fortunately very few events show more than one pair of candidates. Five percent of the sample had two candidate pairs and both of the pairs are included in the comparison. Figure 17 shows a comparison of the accompanying multiplicities for a π^+ beam and Fig. 18 for π^- events. Muon pairs are subtracted from the dimuon event multiplicities while the appropriate two pions are subtracted from the interaction events with which a comparison is made. No statistically significant difference can be observed.

CONCLUSION

In conclusion it is clear that these two experiments utilize their large solid angle coverage and good resolution to produce unique results in spite of very low sensitivity. The electron study produced the first clear evidence that single electrons are not produced in anomalously large quantities but that those observed in other experiments are almost completely due to electron pairs. The streamer chamber experiment makes use of its good resolution to show the first model independent evidence for a mass enhancement below the ρ which is not due to Dalitz decays of known mesons.

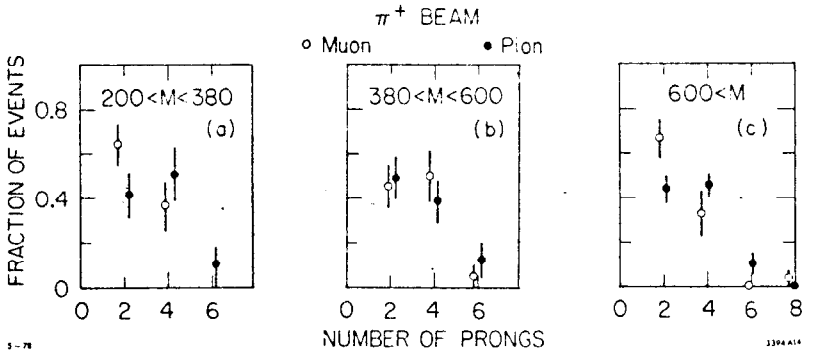

Fig. 17. Accompanying multiplicity distributions for muon pair events and for pairs of pions which are incident on the hadron absorber in an interaction experiment.

$\langle M_{\mu\mu} \rangle = 288$	$\langle M_{\mu\mu} \rangle = 470$	$\langle M_{\mu\mu} \rangle = 864$
$\langle M_{\pi\pi} \rangle = 316$	$\langle M_{\pi\pi} \rangle = 512$	$\langle M_{\pi\pi} \rangle = 882$
$\langle \eta_{\mu\mu} \rangle = 2.71 \pm .2$	$\langle \eta_{\mu\mu} \rangle = 3.2 \pm .28$	$\langle \eta_{\mu\mu} \rangle = 2.83 \pm .27$
$\langle \eta_{\pi\pi} \rangle = 3.30 \pm .3$	$\langle \eta_{\mu\mu} \rangle = 3.27 \pm .26$	$\langle \eta_{\mu\mu} \rangle = 3.31 \pm .14$

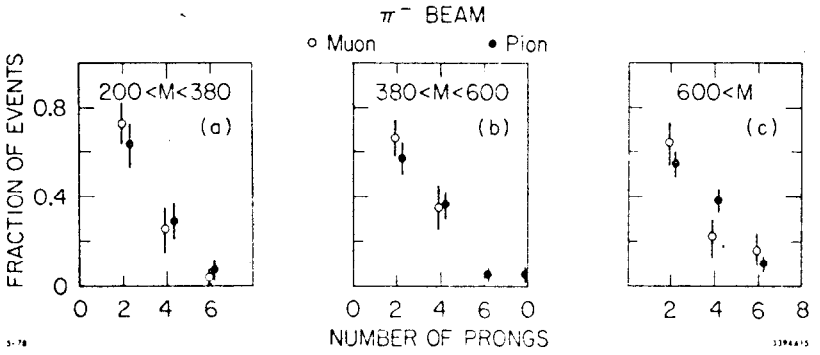

Fig. 18. Accompanying multiplicity distributions for muon pair events and for pairs of pions which are incident on the hadron absorber in an interaction experiment.

$\langle M_{\mu\mu} \rangle = 309$	$\langle M_{\mu\mu} \rangle = 473$	$\langle M_{\mu\mu} \rangle = 788$
$\langle M_{\pi\pi} \rangle = 309$	$\langle M_{\pi\pi} \rangle = 494$	$\langle M_{\pi\pi} \rangle = 895$
$\langle \eta_{\mu\mu} \rangle = 2.63 \pm .2$	$\langle \eta_{\mu\mu} \rangle = 2.69 \pm .2$	$\langle \eta_{\mu\mu} \rangle = 3.05 \pm .26$
$\langle \eta_{\pi\pi} \rangle = 2.88 \pm .22$	$\langle \eta_{\pi\pi} \rangle = 3.09 \pm .18$	$\langle \eta_{\pi\pi} \rangle = 3.12 \pm .10$

REFERENCES

1. J. Bartke et al. Nucl. Phys., B118, 360 (1977).
2. C. H. Lai and C. Quigg, FN-296 (1976); C. Quigg and J. D. Jackson, U.C.R.L.-18487 (1968).
3. J. D. Bjorken and H. Weisberg, Phys. Rev. D13, 1405 (1976).
4. M. Duong-van and R. Blankenbecler, to be published.
5. G. R. Farrar and S. C. Frautschi, Phys. Rev. Lett. 36, 1017 (1976).
6. K. J. Anderson et al., Phys. Rev. Lett. 36, 799 (1976).